MANEUVER TRIM OPTIMIZATION TECHNIQUES FOR ACTIVE AEROELASTIC WINGS

P. Scott Zink*, Dimitri N. Mavris†, Daniella E. Raveh‡
Aerospace Systems Design Laboratory
School of Aerospace Engineering
Georgia Institute of Technology, Atlanta, Georgia, 30332-0150

Abstract

A new method for performing trim optimization of Active Aeroelastic Wing (AAW) technology is presented. The method is based on posing the trim problem as a linear program and solving it with the simplex method. Trim optimization is then integrated with the structural design process in a sequential manner, such that new optimal deflections of the control surfaces are computed for every structural design iteration. The use of the simplex method for trim optimization allowed the elimination of non-physical constraints that had to be imposed when a gradient-based method was used. This resulted in significantly better objectives for the trim optimization. The sequential AAW design process was demonstrated on a lightweight fighter type aircraft performing symmetric and antisymmetric maneuvers at subsonic and supersonic speeds. The concurrent trim and structural optimization resulted in a significantly lighter structure compared to a structure designed with conventional control technology and to a structure employing AAW technology with fixed control surface deflections.

Introduction

An emerging and promising technology for addressing the problem of adverse aeroelastic deformation, such as control surface reversal, is Active Aeroelastic Wing (AAW) technology. It has recently been a key area of study for both the government and industry[1,2] and is defined by Pendleton et. al., as "a multidisciplinary, synergistic technology that integrates air vehicle aerodynamics, active controls, and structures together to maximize air vehicle performance"[3]. AAW technology exploits the use of leading and trailing edge control surfaces to aeroelastically shape the wing, with the resulting aerodynamic forces from the flexible wing becoming the primary means for generating control power. With AAW, the control surfaces then act mainly as tabs and not as the primary sources of control power as they do with a conventional control philosophy. As a result, wing flexibility is seen as an advantage rather than a detriment, since the aircraft can be operated beyond reversal speeds and still generate the required control power for maneuvers. Hence, there is potential for significant reductions in structural weight and actuator power.

Figure 1 illustrates conceptually the differences between AAW technology and a conventional control approach. The hypothetical example shows the cross section of two wings deforming due to aeroelastic effects. The wing on the left, employing AAW technology, is twisting in a positive way with the use of both leading and trailing edge surfaces, while the conventionally controlled wing on the right, which uses only the trailing edge surface, is twisting in a negative way[4]. This adverse twist due to the deflection of the trailing edge surface is associated with reduced control surface effectiveness and control surface reversal in which the increase in camber due to the deflection of the surface is offset by the negative twist of the wing.

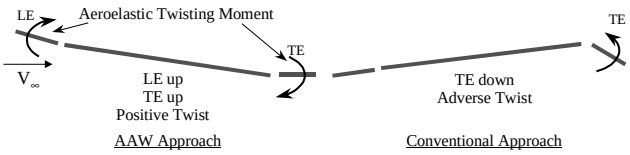

Figure 1 - AAW Technology vs. Conventional Control

Since AAW technology is multidisciplinary in nature, structural design using the technology necessarily requires detailed information about the vehicle structures, aerodynamics, and controls, and in particular, is heavily dependent on control law design, which in turn depends on the flexible structure. As a result, there is a need for an AAW design process in which the structure and control laws are optimized concurrently.

In consideration of AAW technology's use of redundant control surfaces, important constituents of the technology are control surface gear ratios which dictate how one control surface deflects with respect to a single basis surface. Two gear ratio scenarios are illustrated in Figure 2, in which the deflections of the leading edge inboard (LEI), leading edge outboard (LEO), and trailing edge inboard (TEI) surfaces are

---

* Graduate Research Assistant, Student Member AIAA
† Assistant Professor, Senior Member AIAA
‡ Postdoctoral Fellow, Member AIAA

linearly dependent on the deflection of the trailing edge outboard surface (TEO). The gear ratios significantly influence the aeroelastic load distribution, which in turn affects structural response. For the purposes of this research the gear ratios constitute the control laws.

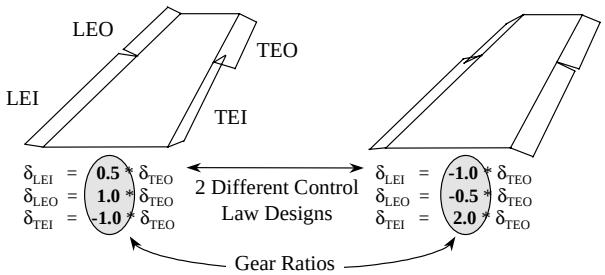

Figure 2 – Gear Ratio Illustration

The *AAW design process* refers to the concurrent optimization of the structure and the gear ratios. Structural optimization refers to the sizing of structural elements (e.g., skin thickness, spar thickness) to minimum weight subject to stress, aeroelastic constraints, etc. Optimization of the gear ratios, more commonly known as trim optimization, is the process of selecting the gear ratios or control surface deflection angles that trim the aircraft to a prescribed maneuver while minimizing some objective function. The need for trim optimization is due to AAW technology's use of redundant control surfaces, which means that the static aeroelastic trim equations cannot be solved in a closed form manner.

Volk and Ausman[5] added a trim optimization capability to ASTROS[6], a finite element based structural optimization code. The trim optimization objective was to minimize the overall control surface actuator command signal or in other terms, control energy. The optimization was performed by using a Newton-Raphson method. A latter version of the program incorporated the ability to also limit the control surface hinge moments[7]. Applications of these trim optimization capabilities in ASTROS can be found in References [8] and [9] in which control surface gearing was studied for rolling maneuvers of a fighter-type aircraft utilizing AAW technology. Similarly, Miller[10] formulated the trim optimization problem as a minimization of a control surface energy function, subject to bending moments, torsion, hinge moments, roll rate, and roll acceleration constraints. The process employed a gradient-based optimization algorithm. As an evolution of Miller's work, Zillmer[11] posed trim optimization as the minimization of a composite function of stress, induced drag, and buckling load. Trim optimization was performed in the Integrated Structure/Maneuver Design (ISMD) program. Stability derivatives that are necessary for trim balance, and sensitivities of the objectives with respect to the control surface deflections, were obtained from a NASTRAN static aeroelastic analysis.

Zillmer[11,12] developed an iterative approach to the AAW design process, in which the trim optimization algorithm implemented in ISMD, discussed above, is imbedded in an iterative process with NASTRAN. The maneuver loads due to the optimized deflections from ISMD are transferred to NASTRAN, which then optimizes the structure to minimum weight. NASTRAN then passes stability derivative and sensitivity information of the current structural design to ISMD for another trim optimization. This process repeats itself until the wing weight converges.

Love et al.[13] proposed a generalized trim capability in which any linear combination of component loads (section bending moment, torsion, hinge moments, etc.) or trim parameters could be the objective of the trim optimization problem. In addition, component loads could be considered as constraints. The optimization problem was solved by a modified method of feasible directions algorithm (MMOFD)[14], which is the optimization algorithm implemented in ASTROS for structural optimization. However, the MMOFD is not the ideal algorithm for solving the trim optimization problem (as will be discussed in more detail in a following section), and this led to the necessity of imposing additional constraints on the problem. The method was implemented in ASTROS so that stability derivatives and sensitivity information were not obtained from an external source. Zink et al.[15] applied the techniques of Reference [13] in a design study of a generic lightweight fighter concept employing AAW technology. Trim optimization was performed for symmetric (pull-up, push-over) and antisymmetric (rolling) maneuvers. The intention was that trim and structural optimization would be repeated iteratively as proposed in Reference [13]. However, only the first step was demonstrated, as trim optimization was performed only once on the starting structural design.

The difficulties with trim optimization in Reference [15] have prompted the authors to explore other means of solving the trim optimization problem. Recognizing that both the symmetric and antisymmetric trim problems are linear, the authors propose that the optimization problem can be posed as a linear program and solved by the simplex method[16,17,18]. Then, the optimal control surface deflections, resulting from trim optimization, are converted to gearing ratios and used in a structural optimization within ASTROS. Following the proposed process of Reference [13], a sequential design process is demonstrated that iterates between trim optimization and structural optimization steps, until the optimal structure with its optimal control surface deflections are obtained. The paper presents a comparison between results of trim optimization

performed with the MMOFD and the simplex algorithms. An AAW design study is performed on a lightweight composite fighter aircraft. The optimal structural design obtained by the sequential AAW design process is then compared to the structural design of an AAW whose control law remains fixed over the course of the structural optimization. In addition, comparison is made to a conventionally controlled wing, indicating some of the weight benefits associated with the use of AAW technology.

Methodology

Static Aeroelastic Equation

The basic equation for the static aeroelastic analysis of a free aircraft by the finite element method in discrete coordinates is[20]:

$$[[K]-q[AICS]]\{u\}+[M][\phi_r]\{\ddot{u}_r\}=[P]\{\delta\} \quad (1)$$

where [K] is the stiffness matrix, [AICS] is the aerodynamic influence coefficients matrix transformed to the structural degrees of freedom, {u} are the displacements and rotations at the structural nodes, [M] is the mass matrix, $[\phi_r]$ are the rigid body modes of the free aircraft, $\{\ddot{u}_r\}$ is a vector of rigid body accelerations, [P] is a matrix of the rigid aerodynamic force coefficients due to aerodynamic trim parameters, q is the dynamic pressure, and $\{\delta\}$ is the aerodynamic trim parameter values (e.g., angle of attack, aileron deflection, steady roll rate). For a free aircraft, Equation (1) is solved together with the following constraint on the elastic displacements[19]:

$$[\phi_r]^T[M]\{u\}=\{0\} \quad (2)$$

Substitution of {u} from equation (1) into Equation (2) yields the trim equation[20]:

$$[L]\{\ddot{u}_r\}=[R]\{\delta\} \quad (3)$$

where [L] is the resultant aeroelastic mass, and [R] is the resultant aeroelastic trim forces. In the case where the number of free trim parameters $\{\delta\}$ is equal to the number of rigid body modes $\{\ddot{u}_r\}$, Equation (3) has a closed form solution. However, if multiple control surfaces (i.e., redundant surfaces) are desired to trim the aircraft, then the closed form solution no longer exists. The trim solution must then be formulated as an optimization problem (i.e., trim optimization) to determine the combination of control surface deflections that trim the aircraft and minimize an objective of interest to the structural designer.

Trim Optimization by MMOFD

Trim optimization by the MMOFD is performed for both symmetric and antisymmetric maneuvers. For the symmetric maneuvers, the trim optimization problem is posed as a minimization of root bending moment (RBM), where the wing control surfaces are used to tailor the load distribution and provide load relief at the wing root, thus ultimately reducing wing weight.

The symmetric trim optimization problem[15] is formally stated as:

Minimize:

$$RBM=\sum_{i=1}^{n_{cs}}\left(\frac{\partial(RBM)}{\partial\delta_i}\right)_{flex}\delta_i+\left(\frac{\partial(RBM)}{\partial\alpha}\right)_{flex}\alpha \quad (4)$$

Subject to: *Control Surface Travel Limits*

$-30^o \le \delta_{LEI} \le 5^o$, $-30^o \le \delta_{LEO} \le 5^o$,
$-30^o \le \delta_{TEI} \le 30^o$, $-30^o \le \delta_{TEO} \le 30^o$,
$-30^o \le \delta_{HT} \le 30^o$, $-10^o \le \alpha \le 30^o$

Hinge Moment (HM) Constraints

$-3.0*10^5 \le HM_{LEI} \le 3.0*10^5$,
$-1.0*10^5 \le HM_{LEO} \le 1.0*10^5$,
$-1.5*10^5 \le HM_{TEI} \le 1.5*10^5$,
$-5.0*10^4 \le HM_{TEO} \le 5.0*10^4$ (lb-in)

where the hinge moment for each control surface (cs) is given by:

$$HM_{cs}=\sum_{i=1}^{n_{cs}}\left(\frac{\partial(HM_{cs})}{\partial\delta_i}\right)_{flex}\delta_i+\left(\frac{\partial(HM_{cs})}{\partial\alpha}\right)_{flex}\alpha+\left(\frac{\partial(HM_{cs})}{\partial a_z}\right)_{flex}a_z \quad (5)$$

Satisfaction of Trim Equations (Lift and Pitching Moment Balance)

$$\sum_{i=1}^{n_{cs}}\left(\frac{\partial L}{\partial\delta_i}\right)_{flex}\delta_i+\left(\frac{\partial L}{\partial\alpha}\right)_{flex}\alpha+L_{const}=ma_z \quad (6)$$

$$\sum_{i=1}^{n_{cs}}\left(\frac{\partial M}{\partial\delta_i}\right)_{flex}\delta_i+\left(\frac{\partial M}{\partial\alpha}\right)_{flex}\alpha+M_{const}=0 \quad (7)$$

Design Variables: α, δ_{LEI}, δ_{LEO}, δ_{TEI}, δ_{TEO}, δ_{HT}

where HT is the horizontal tail, α is the angle of attack, δ_i are the control surface deflections, a_z is the vertical acceleration, m is the aircraft mass, n_{cs} is the number of control surfaces, and L_{const} and M_{const} refer to the lift and moment terms that are not dependent on control surface deflection and angle of attack. The lift and moment derivatives of Equations (6) and (7) are the dimensional flexible stability derivatives, estimated from the trim equation (Equation 3). Similarly, the flexible component load derivatives (∂(RBM)/$\partial\delta$, ∂(HM)/$\partial\delta$) are estimated by multiplying the applied loads (both inertial and aeroelastic) due to a unit deflection of the

trim parameter, by an appropriate matrix that represents the moment arm from each grid point to the section about which the moment is being calculated.

For the antisymmetric maneuvers, trim optimization is formulated as a minimization of the total hinge moments, subject to the surface travel limits, hinge moment constraints, and trim balance requirements, as given formally by:

Minimize: $HM_{LEI} + HM_{LEO} + HM_{TEI} + HM_{TEO}$
Subject to: *Control Surface Travel Limits*
$-30^o \le \delta_{LEI} \le 5^o$, $-30^o \le \delta_{LEO} \le 5^o$,
$-30^o \le \delta_{TEI} \le 30^o$, $-30^o \le \delta_{TEO} \le 30^o$
Hinge Moment Constraints
$-3.0*10^5 \le HM_{LEI} \le 3.0*10^5$,
$-1.0*10^5 \le HM_{LEO} \le 1.0*10^5$,
$-1.5*10^5 \le HM_{TEI} \le 1.5*10^5$,
$-5.0*10^4 \le HM_{TEO} \le 5.0*10^4$ (lb-in)
where the hinge moment for each control surface is:

$$HM_{cs} = \sum_{i=1}^{n_{cs}} \left(\frac{\partial (HM_{cs})}{\partial \delta_i} \right)_{flex} \delta_i + \left(\frac{\partial (HM_{cs})}{\partial p} \right)_{flex} p \quad (8)$$

Satisfaction of Trim Equations
(Roll Moment Balance)

$$\sum_{i=1}^{n_{cs}} \left(\frac{\partial £}{\partial \delta_i} \right)_{flex} \delta_i + \left(\frac{\partial £}{\partial p} \right)_{flex} p = 0 \quad (9)$$

Design Variables: δ_{LEI}, δ_{LEO}, δ_{TEI}, δ_{TEO}

where £ is rolling moment, and p is the user-specified roll rate. The minimization of hinge moments turned out to be difficult, as initially the optimizer would drive the hinge moments to large negative values, which were as bad as large positive values[15]. This is due to the fact that positive (downward) deflection of the trailing edge surfaces produces negative hinge moment. In order to prevent this, for the subsonic rolling maneuver, HM_{TEI} and HM_{TEO} were constrained to be negative, and multiplied by negative one in the objective. For the supersonic rolling maneuver, the trailing edge hinge moments were constrained to be positive, since the trailing edge surfaces were found to be reversing. These difficulties prompted the authors to explore more suitable methods for solving the trim optimization. The next section poses the trim optimization as a linear program to be solved by the simplex method.

Trim Optimization by the Simplex Method

The simplex method[18] is a non-gradient-based algorithm designed for the solution of linear programs. A linear program is an optimization problem whose objective and constraints (inequality and/or equality) are linear functions of the design variables. One of the features of the simplex method is that convergence to the optimal solution is typically very consistent, meaning that regardless of the starting point, the algorithm will converge to the same solution.

The symmetric trim optimization problem, as formulated in the previous section, is already cast in the form of a linear program. The antisymmetric problem, as it is posed, is also a linear program. However, to overcome the difficulties of the MMOFD algorithm driving the hinge moments to large negative values, the antisymmetric trim problem is cast as a minimization of the absolute value of each hinge moment term. The objective function then becomes:

$$F = |HM_{LEI}| + |HM_{LEO}| + |HM_{TEI}| + |HM_{TEO}|$$

One immediately recognizes that this is a nonlinear function, and thus as it is, does not constitute a linear program. However, the absolute value function can be "converted" to linear programming form by defining a new linear objective, e_{cs}, for each hinge moment term and constraining it to be positive, as given by[16]:

Minimize: e_{cs}
Subject to: $e_{cs} \ge HM_{cs}$
$e_{cs} \ge -HM_{cs}$

Thus, e_{cs} is always positive due to the two constraints. If HM_{cs} is positive, then the first constraint is active. If HM_{cs} is negative, then the second constraint is active. Regardless, at all times at least one of the constraints is active. The antisymmetric trim optimization problem, with these new objectives and constraints, then becomes:

Minimize: $e_{LEI} + e_{LEO} + e_{TEI} + e_{TEO}$
Subject to: *Constraints on* e_{cs}

$$-e_{cs} + \sum_{i=1}^{n_{cs}} \left(\frac{\partial (HM_{cs})}{\partial \delta_i} \right)_{flex} \delta_i + \left(\frac{\partial (HM_{cs})}{\partial p} \right)_{flex} p \le 0 \quad (10)$$

$$-e_{cs} - \sum_{i=1}^{n_{cs}} \left(\frac{\partial (HM_{cs})}{\partial \delta_i} \right)_{flex} \delta_i - \left(\frac{\partial (HM_{cs})}{\partial p} \right)_{flex} p \le 0 \quad (11)$$

Control Surface Travel Limits
Hinge Moment Constraints
Satisfaction of Trim Equation

As a result of the constraints in Equations (10) and (11), there are eight more constraints (two for each control surface) in the trim optimization problem, in addition to the original constraints that remain unchanged for the new formulation.

Sequential AAW Design

The sequential AAW design process is performed by iterating between trim optimization, by the simplex method in Matlab[21], and structural optimization by ASTROS, as presented in Figure 3. For each structural optimization iteration, the control surface deflections for the current structural design are optimized. Then, these new control surface deflections are converted to gear ratios (eliminating the redundancies of Equation 3) and passed to the structural optimizer, which then proceeds to take another step. After the structural optimization step, the aeroelastic equations for the new structural design are assembled, and the appropriate stability derivatives, trim objective and constraint coefficients (needed in Equations 4, 5, 6, 7, 8, 9) are calculated in ASTROS and then output to trim optimization. This process repeats itself until the structural optimization objective, wing weight, is converged.

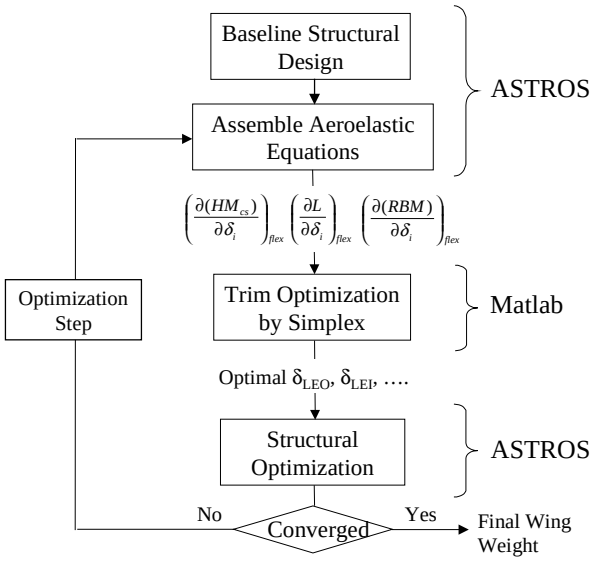

Figure 3 – Sequential AAW Design Process

Results

Structural and Aerodynamic Models

The structural model of the aircraft used both in this research and in Reference [15] is shown in Figure 4. It is an ASTROS preliminary design finite element model of a lightweight composite fighter aircraft with 4 wing control surfaces (2 trailing edge, 2 leading edge) and a horizontal tail[22,23]. It corresponds to a wing with an aspect ratio of 3.0, a total planform area of 330 ft^2, a taper ratio of 20.0%, a leading edge sweep of 38.7°, and a thickness ratio of 3%. The skins of the wing are made up of 4 composite orientations, 0°, ± 45°, and 90° plies, where the thickness of the –45° and +45° orientations are constrained to be equal. The composite wing skin plies are designed (*tailored*) in thickness, via ASTROS optimization routines, to meet specified maneuver and strength requirements.

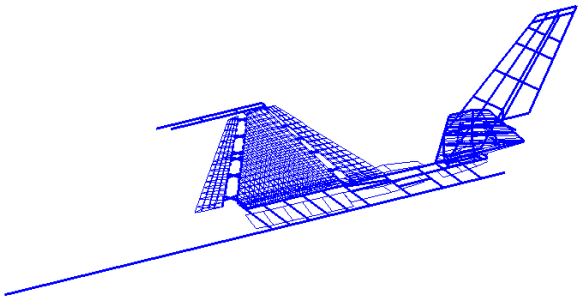

Figure 4 - Structural Model of Generic Fighter

The aerodynamic model is shown in Figure 5. It is a flat panel Carmichael[24] model containing 143 vertical panels and 255 horizontal panels. It also contains paneling for the four wing control surfaces and horizontal tail to coincide with the control surfaces on the structural model. Carmichael aerodynamic influence coefficients are produced for two Mach numbers, 0.95 and 1.2, for both symmetric and antisymmetric conditions[25].

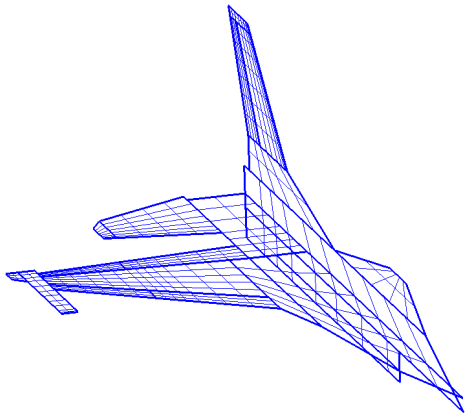

Figure 5- Aerodynamic Model of Generic Fighter

The design variables for structural optimization are the layer thickness of the composite skins. The number of design variables is 78 due to physical linking of the skin elements. Internal structure and carry-thru structure remain fixed. Table 1 shows the maneuver conditions and strength constraints to which the structure is designed.

Table 1 - Maneuver Conditions and Design Constraints

Maneuver Condition	Design Constraint
1) Mach 0.95, 10,000 ft. 9g Pull Up	fiber strain: 3000 με tension 2800 με compression
2) Mach 1.20, Sea Level -3g Push Over	fiber strain: 3000 με tension 2800 με compression
3) Mach 1.20, Sea Level Steady State Roll = 100^{O}/s	fiber strain: 1000 με tension 900 με compression
4) Mach 0.95, 10,000 ft. Steady State Roll = 180^{O}/s	fiber strain: 1000 με tension 900 με compression

Comparison of Simplex Method and MMOFD

For comparison of the MMOFD and simplex algorithms, trim optimization is performed for Maneuver 1 (subsonic, symmetric 9g pull-up), Maneuver 3 (supersonic roll) and Maneuver 4 (subsonic roll). Trim optimization results for the MMOFD are obtained from Reference [15]. Maneuver 2 is omitted from the comparison as trim optimization by the MMOFD for this maneuver was not performed in Reference [15]. Table 2 shows a comparison of the final results of the two methods for the subsonic rolling maneuver. For trim optimization by the MMOFD the leading edge surfaces were fixed to zero, and the hinge moments for each of the leading edge surfaces were not considered in the objective. As a result, to compare the MMOFD and the simplex method fairly, trim optimization by the simplex method was first posed to reflect the formulation of the MMOFD. The results of this are in the second column, with the simplex method results matching closely the results of the MMOFD. Trim optimization by the simplex method was then performed without the restriction on the leading edge surfaces and hinge moments. The results of this optimization are shown in the third column of Table 2, showing that the removal of these restrictions results in a significantly lower total hinge moment.

Table 2 – Trim Optimization Comparison for Subsonic Roll

	MMOFD	Simplex (like MMOFD)	Simplex
δ_{LEI}	0.000º	0.000º	2.565º
δ_{LEO}	0.000º	0.000º	5.000º
δ_{TEI}	-1.157º	-1.155º	-0.960º
δ_{TEO}	9.457º	9.442º	8.854º
HM_{LEI} (lb-in)	-25566.0	-25560.0	0.000
HM_{LEO} (lb-in)	-23394.0	-23389.0	-4720.0
HM_{TEI} (lb-in)	-0.169	0.000	0.000
HM_{TEO} (lb-in)	-13325.8	-13204.4	-12200.0
Total Objective	62286.0	62153.0	16920.0

Table 3 shows a comparison of the MMOFD and the simplex method for the solution of the supersonic antisymmetric trim problem. In the case of the MMOFD, the trailing edge hinge moments were constrained to be positive, and once again, in the interest of fairness, an optimization by the simplex method was performed to reflect the formulation of the MMOFD. Both methods produce comparable results, with the simplex converging to a slightly lower total hinge moment. However, without the restriction on the trailing edge hinge moments being positive, the simplex method uses more of the TEO surface, resulting in a significantly lower objective (Column 3).

Table 3 – Trim Optimization Comparison for Supersonic Roll

	MMOFD	Simplex (like MMOFD)	Simplex
δ_{LEI}	2.792º	2.792º	0.773º
δ_{LEO}	5.000º	5.000º	2.780º
δ_{TEI}	0.255º	0.414º	0.245º
δ_{TEO}	1.605º	1.603º	13.220º
HM_{LEI} (lb-in)	82610.0	82600.0	0.000
HM_{LEO} (lb-in)	85280.0	85265.0	13870.0
HM_{TEI} (lb-in)	866.0	0.000	0.000
HM_{TEO} (lb-in)	0.150	0.000	-50000.0
Total Objective	168756.2	165200.0	63870.0

The results of the trim optimization for the subsonic, symmetric maneuver are shown in Table 4. A comparison of the two methods shows good agreement in the final converged solution, with the simplex converging to a slightly lower RBM. In addition, the final solution by the simplex method results in a much 'tighter' constraint value for HM_{LEI}, where it fell precisely on its upper limit. This a beneficial characteristic of the simplex method where the optimal solution must lie on a constraint vertex. However, with gradient-based methods, such as the MMOFD, the solution depends heavily on optimization

parameters such as move limits and starting point. In complex problems, there is then no guarantee that the global optimum is reached.

Table 4 – Trim Optimization Comparison for Subsonic Pull-Up

	MMOFD	Simplex
δ_{LEI}	-16.800º	-10.599
δ_{LEO}	-30.000º	-30.000º
δ_{TEI}	-2.140º	0.463º
δ_{TEO}	-30.000º	-30.000º
δ_{HT}	1.902º	2.698º
α	13.032º	12.659º
HM_{LEI} (lb-in)	252230.0	300000.0
HM_{LEO} (lb-in)	100430.0	100000.0
HM_{TEI} (lb-in)	8020.0	-1480.0
HM_{TEO} (lb-in)	40380.0	39920.0
RBM (lb-in)	4372700.0	4351100.0

Overall, the simplex method proved to be better suited for the trim optimization problem as it has been formulated. The simplex solutions, when posed to reflect the MMOFD formulations, converged to slightly better solutions, and were more precise in their satisfaction of the constraints. However, the benefits of the simplex method become even more dramatic when the restrictions of the MMOFD are removed, as is evident in the antisymmetric maneuvers.

Sequential AAW Design Process

The sequential AAW design process, as proposed in Figure 3, was implemented for the ASTROS optimization model discussed earlier. In addition, three other structural optimizations were performed as a basis of comparison to the sequential process. The first of these, identified as AAW Optimization 1, is an ASTROS structural optimization with the optimal control surface deflections for the starting structural design converted to gear ratios that relate the deflection of the dependent control surfaces to the independent (i.e., basis) surfaces. Over the course of the structural optimization these gear ratios remain fixed, and the deflections of the independent surfaces are constrained so that none of the surfaces exceed their allowable travel limits. The independent surfaces and dependent surfaces for each maneuver are given in Table 5.

Table 5 - Independent and Dependent Control Surfaces

	Independent (Basis) Surface	Dependent Surfaces
Maneuver 1	HT	LEI, LEO, TEI, TEO
Maneuver 2	HT	LEI, LEO, TEI, TEO
Maneuver 3	LEO	LEI, TEI, TEO
Maneuver 4	TEO	LEI, LEO, TEI

The second comparison case, identified as AAW Optimization 2, is a structural optimization where the dependent surfaces are set to their optimized deflections for the starting structural design and remain fixed over the course of the structural optimization. The independent surfaces remain free during the optimization, deflecting to achieve the prescribed maneuver requirements. For example, for Maneuver 1, the deflections of the LEI, LEO, TEI, and TEO surfaces remain fixed at their initial optimal values, and the deflection of the horizontal tail and angle of attack remain free to trim the aircraft to a vertical acceleration of 9 g's and zero pitching moment.

The final comparison case is structural optimization for a conventionally controlled aircraft, which would be reflective of how current fighter aircraft are controlled. In this case, only the horizontal tail is used to trim the aircraft for the symmetric maneuvers. For the supersonic antisymmetric maneuver, a blending of the inboard trailing edge surface and horizontal tail (similar to the F-16) is used to achieve the required roll rate, and for the subsonic antisymmetric maneuver, the outboard trailing edge is used. In addition, control surface effectiveness constraints are added to the structural optimization for the antisymmetric maneuvers, as is typically done for modern fighter aircraft that require high roll rates or fast time-to-bank.

The final optimized weights for the sequential AAW design process and the three comparison cases are shown in Table 6. By examination of the weights alone, one observes the benefit that is achieved by performing trim optimization for each iteration of the structural optimization. AAW Optimization 1 employs AAW technology, but since all of the dependent surfaces are geared to the independent surfaces, the independent surfaces have very little "freedom" with which to trim the aircraft. As a result, additional stiffness is added to make the independent surfaces more effective, resulting in an even higher weight than a configuration employing conventional control technology. AAW Optimization 2 results in a lower weight solution simply because the independent surfaces are not "attached" to the dependent surfaces and thus have far more freedom with which to trim the aircraft. However, the weight is not nearly as low as the sequential process, again emphasizing the need to optimize the control surface deflections for each structural design (i.e., at each optimization iteration).

Table 6 - Final Weights for each Optimization

Optimization Case	Weight (lb)
AAW Sequential	292.271
AAW Optimization 1	405.134
AAW Optimization 2	355.50
Conventional Control	383.04

Table 7 – Final Control Surface Deflections and Trim Objective for Subsonic Pull-Up

	Sequential	AAW Optimization 1	AAW Optimization 2	Conventional
δ_{LEI}	-4.609º	-5.990º	-6.350º	0.000º
δ_{LEO}	-30.056º	-28.286º	-30.000º	0.000º
δ_{TEI}	-6.446º	-3.231º	-3.430º	0.000º
δ_{TEO}	-30.056º	-28.286º	-30.000º	0.000º
δ_{HT}	0.790º	1.430º	1.383º	-4.799º
α	11.751º	11.784º	11.699º	10.072º
RBM (lb-in)	4701820.0	4614680.0	4629120.0	6238330.0

Tables 7, 8, 9, and 10 show the control surface deflections and trim optimization objective for the final structural iteration of each of the four optimization cases. Table 7 contains the final data for the subsonic, pull-up maneuver, where one clearly sees the benefit of using the wing control surfaces to relieve RBM. For all three AAW cases, the outboard control surfaces deflect to their largest negative allowable, which for the leading edge surface is nose-down and for the trailing edge surface is tail-up. This has the effect of decreasing the effective angle of attack on the outboard section of the wing, shifting aerodynamic load further inboard, and hence reducing RBM. The three AAW optimization cases result in a 25% reduction in RBM over the conventional control approach. Moreover, in the AAW cases the horizontal tail deflects much less than in the conventional control case. This leads to less tail loading which would contribute to the reduction of structural weight if the tail structure was included in the structural optimization.

Figure 6 is a history of the subsonic, pull-up maneuver control surface deflections after each structural optimization step of the sequential AAW design process, giving an indication of how the control law evolves as the structural design changes. The dashed line on each plot corresponds to the final deflections for AAW Optimization 2. It is seen that the gear ratios significantly change as the structure is

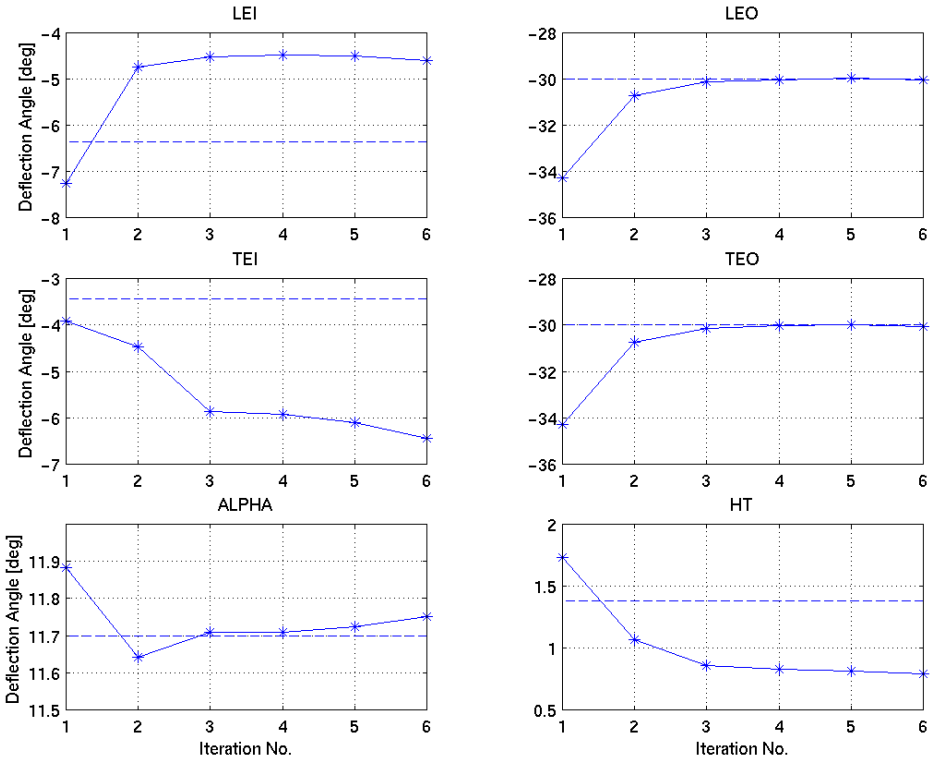

Figure 6 - Control Surface Deflection History (Maneuver 1)

Table 8 - Final Control Surface Deflections and Trim Objective for Supersonic Push-Over

	Sequential	AAW Optimization 1	AAW Optimization 2	Conventional
δ_{LEI}	4.998º	4.499º	5.000º	0.000º
δ_{LEO}	4.998º	4.499º	5.000º	0.000º
δ_{TEI}	-29.290º	-26.005º	-28.900º	0.000º
δ_{TEO}	15.480º	13.537º	15.040º	0.000º
δ_{HT}	2.695º	2.603º	2.660º	2.217º
α	-2.213º	-2.152º	-2.210º	-1.600º
RBM (lb-in)	-1328030.0	-1406360.0	-1324950.0	-2111000.0

optimized, indicating the importance of conducting a concurrent trim and structural optimization.

Table 8 presents the final trim data for the supersonic, push-over maneuver. Here, once again, one observes the dramatic reduction in the magnitude of RBM for the AAW approaches over a conventional approach. In this case, the leading edge surfaces deflect to their largest positive allowables, which is exactly the opposite trend of Maneuver 1. This is due to the fact that Maneuver 2 is a push-over maneuver, hence RBM is naturally negative, and the goal of trim optimization is to increase RBM. This is achieved by maximal upward deflection of the leading edge surfaces. Although, the trailing edge surfaces deflect to rather large values, their ineffectiveness at supersonic speeds results in them having little effect on the RBM, and thus they are used primarily to meet the hinge moment constraints.

Table 9 - Final Control Surface Deflections and Trim Objective for Supersonic Roll

	Sequential	AAW Optimization 1	AAW Optimization 2	Conventional
δ_{LEI}	0.705º	0.714º	0.715º	0.000º
δ_{LEO}	4.732º	4.995º	5.000º	0.000º
δ_{TEI}	0.033º	0.115º	0.115º	16.503º
δ_{TEO}	1.093º	11.533º	11.547º	0.000º
HM_{total} (lb-in)	48991.7	82156.0	80488.1	115045.1

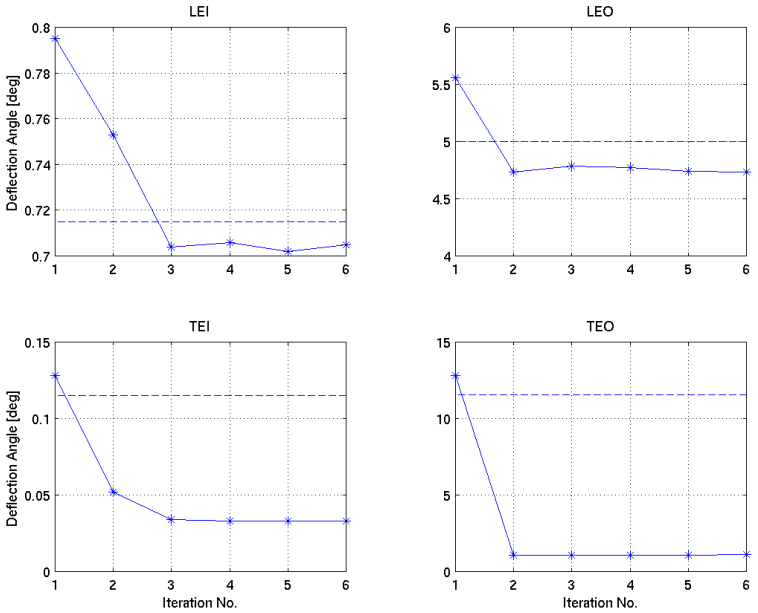

Figure 7 - Control Surface Deflection History (Maneuver 3)

Table 10 - Final Control Surface Deflections and Trim Objective for Subsonic Roll

	Sequential	AAW Optimization 1	AAW Optimization 2	Conventional
δ_{LEI}	3.165º	2.774º	2.774º	0.000º
δ_{LEO}	5.016º	4.989º	5.000º	0.000º
δ_{TEI}	-2.385º	-1.527º	-1.530º	0.000º
δ_{TEO}	15.291º	10.753º	12.064º	14.797º
HM_{total} (lb-in)	39330.9	28369.3	32859.5	90971.1

Table 9 presents the final data for the supersonic, rolling maneuver. The significantly lower value of total hinge moment for the sequential process shows the benefit of performing trim optimization after every iteration, as opposed to letting the gear ratios (AAW Optimization 1) or control surface deflections (AAW Optimization 2) remain fixed over the course of the structural optimization. Examination of the final control surface deflections for each of the three AAW optimization cases reveals that as the structure gets lighter, the trailing edge surfaces are used less and less to achieve the required roll rate. This is made apparent by the lower deflection of the trailing edge surfaces for the sequential approach compared to the other AAW optimization cases. In AAW Optimization 1 and 2 the TEO surface is used rather extensively, as these cases correspond to the optimal control laws for the *starting structural design*, but as is evident by the higher total hinge moment, they are not optimal for the final structural design.

This point is also reinforced in Figure 7 which is a plot of the control surface deflections for each iteration of the sequential AAW design process. The dashed line on each plot refers to the final control surface deflection of AAW Optimization 2. One sees that after the first iteration, usage of the outboard trailing edge surface drops off dramatically. This is due to the fact that from Iteration 1 to Iteration 2 the outboard trailing edge control surface begins to reverse, and hence the trim optimization de-emphasizes this surface in favor of the leading edge surfaces. However, both AAW Optimization 1 and 2 are forced to use this surface as they employ the starting optimal control law, and as a result, pay a rather significant penalty in hinge moment because of its heavy use.

Finally, Table 10 contains the final trim data for the subsonic rolling maneuver. In contrast to the supersonic rolling maneuver, the TEO surface is used rather heavily. This is due to the fact that at the subsonic Mach number, this surface is still effective. Although the total hinge moment by the sequential process is higher than either of the other two AAW optimization cases, the structure is much lighter and more flexible. Thus, the loads acting on this structure produce higher hinge moments. Also, note the significant reduction in total hinge moment when the leading edge surfaces are employed as seen by comparing the AAW cases to the conventional control design.

Conclusion

Trim optimization for Active Aeroelastic Wing technology has been performed using the simplex method and compared against previous trim optimization results that were generated using a gradient-based modified method of feasible directions. The results of this comparison revealed that the simplex method converged to comparable or better solutions and was better suited for the type of trim optimization problems being solved, whose constraints and objectives were linear functions of the design variables. Trim optimization by the simplex method was then integrated into the sequential AAW design process, in which structural optimization and trim optimization are repeated in an iterative fashion. Comparison of final results of the sequential process with a conventional control case demonstrated significant weight savings with the use of AAW technology. In addition, the study showed the benefit of optimizing the control law after each structural iteration by comparing the sequential process to AAW designs based on fixed control laws.

Acknowledgments

The authors extend thanks to Prof. Moti Karpel and Dr. Boris Moulin of Technion-Israel Institute of Technology for their technical advice and assistance on ASTROS. In addition, the authors thank Mr. Michael Love of Lockheed Martin Tactical Aircraft Systems for his involvement in trim optimization by the modified method of feasible directions.

References

1) Miller, G.D., "Active Flexible Wing (AFW) Technology," Air Force Wright Aeronautical Laboratories, TR-87-3096, February 1988.

2) Perry III, B., Cole, S.R., and Miller, G.D., "A Summary of an AFW Program," Journal of Aircraft, Vol. 32, No. 1, January-February 1995, pp. 10-15.

3) Pendleton, E., Griffin, K., Kehoe, M., and Perry, B., "A Flight Research Program for Active Aeroelastic Wing Technology," 37th AIAA/ ASME/ ASCE/ AHS/ ASC Structures, Structural Dynamics, and Materials Conference, Salt Lake City, UT, April 15-17, 1996.

4) Flick, P.M., Love, M.H., and Zink, P.S., "The Impact of Active Aeroelastic Wing Technology on Conceptual Aircraft Design," NATO Research and Technology Agency, Proceedings of the Applied Vehicle Technology Panel Fall 1999 Meeting, Ottawa, Canada, October 1999.

5) Volk, J., and Ausman, J., "Integration of a Generic Flight Control System into ASTROS," 36th AIAA/ ASME/ASCE/AHS/ASC Structures, Structural Dynamics, and Materials Conference, Salt Lake City, UT, April 15-17, 1996, AIAA-96-1335.

6) Neill, D.J., Johnson, E.H., and Canfield, R., "ASTROS-A Multidisciplinary Automated Design Tool," Journal of Aircraft, Vol. 27, No. 12, 1990, pp. 1021-1027.

7) Ausman, J., and Volk, J., "Integration of Control Surface Load Limiting into ASTROS," 38th AIAA/ ASME/ASCE/AHS/ASC Structures, Structural Dynamics, and Materials Conference, Kissimmee, FL, April 7-10, 1997, AIAA-97-1115.

8) Forster, E., Kolonay, R., Venkayya, V. and Eastep, F., "Optimization of a Generic Fighter Wing Incorporating Active Aeroelastic Wing Technology," 6th AIAA/NASA/ISSMO Symposium on Multidisciplinary Analysis and Optimization, Bellevue, WA, September 1996.

9) Anderson, G., Forster, E., Kolonay, R., and Eastep, F., "Multiple Control Surface Utilization in Active Aeroelastic Wing Technology," Journal of Aircraft, Vol. 34, No. 4, 1997, pp. 552-557.

10) Miller, G.D., "An Active Flexible Wing Multi-Disciplinary Design Optimization Method," 5th AIAA/ USAF/NASA/ISSMO Symposium on Multidisciplinary Analysis and Optimization, Panama City, FL, September 7-9, 1994, AIAA-94-4412.

11) Zillmer, S., "Integrated Multidisciplinary Optimization for Active Aeroelastic Wing Design," Air Force Wright Aeronautical Laboratories, WL-TR-97-3087, August 1997.

12) Dobbs, S.K., Schwanz, R.C., and Abdi, F., "Automated Structural Analysis Process at Rockwell," Integrated Airframe Design Technology, Presented at 82nd Meeting of the AGARD Structures and Materials Panel, Sesimbra, Portugal, May 8-9, 1996, AGARD Report 814.

13) Love, M.H., Barker, D.K., Egle, D.D., Neill, D.J., and Kolonay, R.M., "Enhanced Maneuver Airloads Simulation for the Automated Structural Optimization System – ASTROS," 38th AIAA/ ASME/ ASCE/ AHS/ ASC Structures, Structural Dynamics, and Materials Conference, Kissimmee, FL, April 7-10, 1997.

14) Vanderplaats, G.N., and Moses, F., "Structural Optimization by Methods of Feasible Directions," Journal of Computers and Structures, Vol. 3, July 1973, pp. 739-755.

15) Zink, P.S., Mavris, D.N., Flick, P.M., and Love, M.H., "Impact of Active Aeroelastic Wing Technology on Wing Geometry using Response Surface Methodology," CEAS/AIAA/ICASE/NASA Langley International Forum on Aeroelasticity and Structural Dynamics, Williamsburg, VA, June 22-25, 1999.

16) Chvátal, V., Linear Programming, W.H. Freeman and Company, New York, 1983.

17) Vanderplaats, G.N., Numerical Optimization Techniques for Engineering Design: With Applications, McGraw-Hill, Inc., New York, 1984.

18) Dantzig, G.B., Orden, A., Wolfe, P., "The Generalized Simplex Method for Minimizing a Linear Form under Linear Inequality Restraints," Pacific Journal of Mathematics, Vol. 5, 1955, pp. 183 – 195.

19) Rodden, W.P., and Love, J.R., "Equations of Motion of Quasisteady Flight Vehicle Utilizing Restrained Static Aeroelastic Characteristics," Journal of Aircraft, Vol. 22, No. 9, September 1995, pp. 802–809.

20) Johnson, E.H., and Venkayya, V.B., ASTROS Theoretical Manual, AFWAL-TR-88-3028, December 1988.

21) MathWorks, Inc., Using MATLAB – Version 5, 1996.

22) Karpel, M., Moulin, B., and Love, M.H., "Modal-Based Structural Optimization with Static Aeroelastic and Stress Constraints," Journal of Aircraft, Vol. 34, No. 3, 1997, pp.433-440.

23) Zink, P.S., Mavris, D.N., Love, M.H., and Karpel, M., "Robust Design for Aeroelastically Tailored/Active Aeroelastic Wing," 7th AIAA/USAF/NASA/ISSMO Symposium on Multidisciplinary Analysis and Optimization, St. Louis, MO, September 2-4, 1998, AIAA-98-4781.

24) Carmichael, R.L., Castellano, C.R., and Chen, C.F., The Use of Finite Element Methods for Predicting the Aerodynamics of Wing-Body Combinations, NASA SP-228, October 1969.

25) Barker, D.K. and Love, M.H., "An ASTROS Application with Path Dependent Results," AIAA/USAF/NASA/ISSMO Multidisciplinary Analysis and Optimization Conference, Bellevue, WA, September 1996.